IJCRT.ORG ISSN : 2320-2882

INTERNATIONAL JOURNAL OF CREATIVE RESEARCH THOUGHTS (IJCRT)

An International Open Access, Peer-reviewed, Refereed Journal

DESIGN AND ANALYSIS OF WHEEL ASSEMBLY FOR STAMPING, CHARGING, & PUSHING MACHINE IN COKE PLANT.

[1]Asst Prof. Mr. AJAY KUMAR D, [2]Mr. AKHIL V, [3]MANI SHANKAR G, [4]KANAKA RAJU P, [5]ASHOK KUMAR D

[1]Asst Prof, [2]Student(20551A0357), [3]Student(20551A0309), [4]Student(20551A0335), [5]Student(20551A0364),

MECHANICAL ENGINEERING,

GODAVARI INSTITUTE OF ENGINEERING AND TECHNOLOGY(AUTONOMOUS), RAJAHMAHENDRAVARAM

Abstract: The SCP Machine serves the purpose of stamping coking coal into cake, charging it into the oven, and pushing out the resulting coke. The machine's long travel involves 8 double-wheeled bogies, with one serving as the drive wheel and the others as driven wheels. These wheels are interference fitted onto their shafts. The drive wheel sets have shaft extensions with hollow shaft gear boxes attached using shrink disc assemblies. Upon dismantling a broken shaft, it was observed that a cup and cone shape had formed in the middle, and the outer surface was severely rubbed during rotation leading to the failure. The space between the shaft and the DE side bearing showed significant wear and deformation due to rotation. The shaft and DE side bearing were sent to a scientific lab for material analysis. While moving the wheels with some load, the wheel shafts were found to get damaged, prompting an investigation to identify the issues causing the breakage under various conditions. The design and analysis of the wheel and shaft assembly were carried out using CREO & ANSYS Software, complemented by manual calculations in MS Excel.

Keywords: CREO Parametric 8.0.2.0, ANSYS Workbench 2021 R2, MS Excel

I. Introduction

The SCP machine, responsible for stamping, charging, and pushing, is monitored by the Ram Side Machine Maintenance Section. It features three main mechanisms—stamping, charging, and pushing. Stamp-charging technology, a modern and proven cooking method, meets environmental requirements globally. It enables the production of high-quality coke from a variety of charge coals, including low-rank coals, petroleum coke, and coke breeze. The SCP machine's function involves stamping coking coal into cake, charging it into the oven, and pushing the resulting coke out. The SCP machine's long travel includes 8 double-wheeled bogies with one drive wheel and another as a driven wheel, with interference-fitted wheels on their shafts. Drive wheel sets are equipped with shaft extensions, and hollow shaft gear boxes are attached using shrink disc assemblies.

2)LITERATURE REVIEW:

In 1995 Prasad HN et al., [1] Proposed a Role of stamped charging in utilizing non coking coals for coke making. This article presents a Stamp-Charged Coke-Making Technology. Stamp-Charged Coke-Making Technology-The Effect of Charge Density and the Addition of Semi-soft coals on the Structural, Textural and Quality Parameters of Coke To make the properties of the Stamp-Charging coke-making Elements And maintaining the perfect dimensions And Accurate Shape.

Carl Lindgren et al., [2] in 1983 Presented a Cake oven charging car. Flat push coke wet quenching apparatus and process Method and apparatus for coal and coking testing coal coking properties Reduced output rate coke oven operation with gas sharing providing extended process cycle and Systems, methods for improving quenched coke recovery.

Stanca., M., Stefanini, A., Gallo, R. et al., [3] in 2001 Development of an Integrated Design Methodology for a New Generation of High-performance Rail Wheelsets.

J Stratmann et al., [4] in 1972 Proposed the Method and Apparatus for the Evacuation of Coke from a Furnace Chamber. Apparatus for quenching, screening, and loading coke. quenching coke from horizontal coke ovens separating and discharging coke. A specialized transport vehicle designed specifically for receiving coke charges, particularly in conjunction with coke oven batteries.

DG Ullam et al., [5] in 2003 Proposed the Factor of Safety as a Design Variable. Factors of safety, design margins, conservatism, prudence – these are all protective instruments, used to reduce the risk of dangers caused by failure. Protective measures like factors of safety, design margins, conservatism, and prudence are employed to minimize the risks associated with potential failures. The magnitude of factors of safety varies depending on the specific condition under consideration. For instance, the factor of safety used to establish the design limit load based on the flight limit load typically falls within the range of 1.4–1.5. Meanwhile, the factor of safety utilized to determine the ultimate load from the design limit load typically lies between 1.25–1.5.

3) DESIGN PPROCESS:

Flow Chart: Design Process

6) DESIGN OF SHAFT

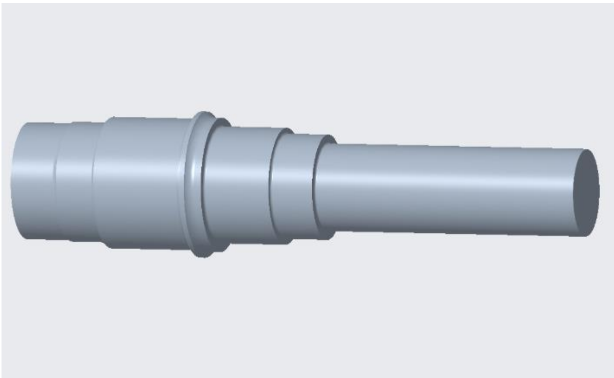

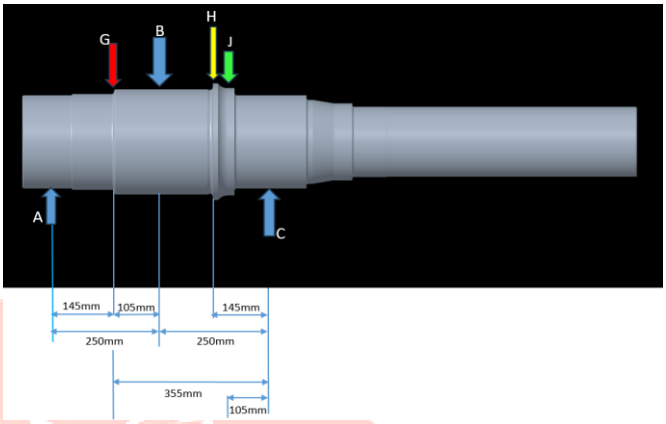

Figure-3: Forced Applied at six Specific Locations along the Shaft

D) Performing Design Calculations for the SCP machine Wheel Assembly Study:

a) SECTION-A

SHEAR FORCE AT POINT- A (SF) = 512.0495KN
BENDING MOMENT AT POINT - A (BM) = 0 **[Formula: M=Force * Length]**
DIAMETER (D) = 200mm
YIELD STRENGTH (Y) = **[Formula: Y=D/2]**
Y= 100mm
MOMENT OF INERTIA (I) = **[Formula: $I = \frac{\pi}{64} * D^4$]**
I = 78539816.34mm^4
BENDING STRESS (σA) = **[Formula: $\sigma A = M * \frac{Y}{I}$]**
σA = 0
SHEAR STRESS (τ) = **[Formula: τ = F/A]**
Shear stress τ = 16.29904195 N/mm^2 and the Bending Stress is σA = 0.

b) SECTION-G

SHEAR FORCE AT POINT- G (SF) = 512.0495KN
BENDING MOMENT AT POINT - G (BM) = **[Formula: M=Force * Length]**
M=Force * Length
M=128012376.1 N/mm^2
DIAMETER (D) = 205mm
YIELD STRENGTH (Y) = **[Formula: Y=D/2]**
Y= 102.5mm
MOMENT OF INERTIA (I) = **[Formula: $I = \frac{\pi}{64} * D^4$]**
I = 86693261.7mm^4
BENDING STRESS (σG) = **[Formula: $\sigma G = M * \frac{Y}{I}$]**
σG = 151.3528N/mm^2
SHEAR STRESS (τ) = **[Formula: τ = F/A]**
Shear stress τ = 15.51366277N/mm^2 and the Bending Stress is σG =151.3528N/mm^2.

c) SECTION-B

SHEAR FORCE AT POINT- B (SF) = 512.0495KN
BENDING MOMENT AT POINT - B (BM) = **[Formula: M=Force * Length]**
M=Force * Length
M= 128012376.1N/mm^2
DIAMETER (D) = 225mm
YIELD STRENGTH (Y) = **[Formula: Y=D/2]**
Y= 112.5mm
MOMENT OF INERTIA (I) = **[Formula: $I = \frac{\pi}{64} * D^4$]**
I = 125805599.4mm^4
BENDING STRESS (σB) = **[Formula: $\sigma B = M * \frac{Y}{I}$]**
σB = 114.473381mm^2
SHEAR STRESS (τ) = **[Formula: τ = F/A]**
Shear stress τ = 12.87825536N/mm^2 and the Bending Stress is σB =114.473381N/mm^2.

d) SECTION-H

SHEAR FORCE AT POINT- H (SF) = 512.0495KN
BENDING MOMENT AT POINT - H (BM) = **[Formula: M=Force * Length]**
M=Force * Length

M=74247178.13N/mm^2
DIAMETER (D) = 250mm
YIELD STRENGTH (Y) = **[Formula: Y=D/2]**
Y= 125mm
AREA (A) = **[Formula: $A = \frac{\pi}{4} * D^2$]**
A= 49087.38527mm^2
MOMENT OF INERTIA (I) = **[Formula: $I = \frac{\pi}{64} * D^4$]**
I = 191747598.5mm^4
BENDING STRESS (σH) = **[Formula: $\sigma H = M * \frac{Y}{I}$]**
$\sigma H = 48.40163496 N/mm^2$
SHEAR STRESS (τ) = **[Formula: τ = F/A]**
Shear stress τ = 10.43138685N/mm^2 and the Bending Stress is σH =48.40163496N/mm^2.

e) SECTION-J

SHEAR FORCE AT POINT- J (SF) = 512.0495KN
BENDING MOMENT AT POINT - J (BM) = **[Formula: M=Force * Length]**
M=53765197.96N/mm^2
DIAMETER (D) = 200mm
YIELD STRENGTH (Y) = **[Formula: Y=D/2]**
Y= 100mm
AREA (A) = **[Formula: $A = \frac{\pi}{4} * D^2$]**
A= 31415.92654mm^2

E) Calculating the Torsional Shear Stress and Polar moment of Inertia

a) SECTION-G

Diameter at G (DG) = 205mm
Polar moment of inertia (JG) = **[Formula: $JG = \frac{\pi}{32} * (DG)^4$]**
JG = 173386523.4mm^4
Radius (r) = **[Formula: r = DG/2]**
r = 102.5mm
Torsional Shear Stress (τG) = **[Formula: τG = T*r / JG]**
τG = 13.57198203N/mm^2.

b) SECTION-B

Diameter at B (DB) = 225mm
Polar moment of inertia (JB) = **[Formula: $JB = \frac{\pi}{32} * (DB)^4$]**
JB = 251611198.7mm^4
Radius (r) = **[Formula: r = DB/2]**
r = 112.5mm
Torsional Shear Stress (τB) = **[Formula: τB = T*r / JB]**
τB = 10.26496103N/mm^2.

c) SECTION-H

Diameter at H (DH) = 230mm
Polar moment of inertia (JH) = **[Formula: $JH = \frac{\pi}{32} * (DH)^4$]**
JH = 274733259.3mm^4
Radius (r) = **[Formula: r = DH/2]**
r = 115mm
Torsional Shear Stress (τH) = **[Formula: τH = T*r / JH]**
τH = 0.009609955N/mm^2

d) SECTION-J

Diameter at J (DJ) = 200mm

MOMENT OF INERTIA (I) = **[Formula: $I = \frac{\pi}{64} * D^4$]**
I = 78539816.34mm^4
BENDING STRESS (σJ) = **[Formula: $\sigma J = M * \frac{Y}{I}$]**
$\sigma J = 68.45597617 N/mm^2$
SHEAR STRESS (τ) = **[Formula: τ = F/A]**
Shear stress τ = 16.29904195N/mm^2 and the Bending Stress is σJ =68.45597617N/mm^2.

f) SECTION-C

SHEAR FORCE AT POINT- C (SF) = 512.0495KN
BENDING MOMENT AT POINT - C (BM) = 0 [**Formula: M=Force * Length]**
DIAMETER (D) = 200mm
YIELD STRENGTH (Y) = **[Formula: Y=D/2]**
Y= 100mm
AREA (A) = **[Formula: $A = \frac{\pi}{4} * D^2$]**
A= 31415.92654mm^2
MOMENT OF INERTIA (I) = **[Formula: $I = \frac{\pi}{64} * D^4$]**
I = 78539816.34mm^4
BENDING STRESS (σC) = 0 [**Formula: $\sigma J = M * \frac{Y}{I}$]**
SHEAR STRESS (τ) = **[Formula: τ = F/A]**
Shear stress τ = 16.29904195N/mm^2 and the Bending Stress is σC =0N/mm^2.

Polar moment of inertia (JJ) = **[Formula: $JJ = \frac{\pi}{32} * (DJ)^4$]**
JJ = 157079632.7mm^4
Radius (r) = **[Formula: r = DJ/2]**
r = 100mm
Torsional Shear Stress (τJ) = **[Formula: τJ = T*r / JJ]**
τJ = 14.61554021N/mm^2.

e) SECTION-C

Diameter at C (DC) = 150mm
Polar moment of inertia (JC) = **[Formula: $JC = \frac{\pi}{32} * (DC)^4$]**
JC = 49700977.53mm^4
Radius (r) = **[Formula: r = DC/2]**
r = 75mm
Torsional Shear Stress (τC) = **[Formula: τC = T*r / JC]**
τC = 34.64424347N/mm^2.

F) DESIGN OF WHEEL:

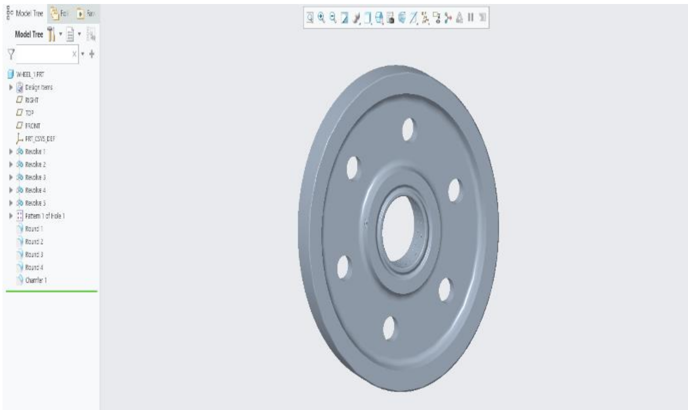

Figure -2: Complete view of the Wheel Modelling

G) ANALYSIS:

a) **Based on the mode of failure, following why-why analysis was carried out to arrive at the root cause:**

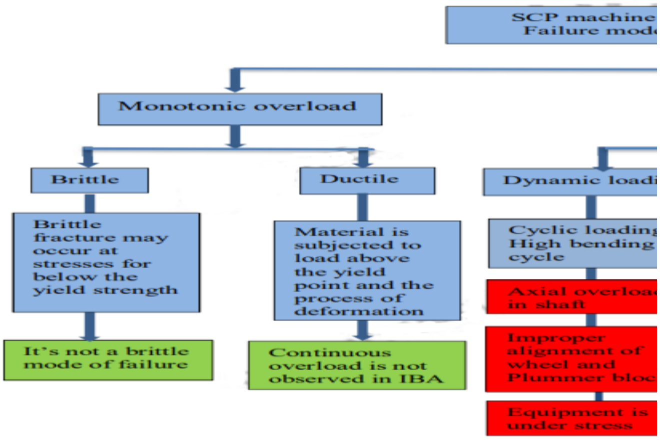

b) **FINITE ELEMENT ANALYSIS:**

i) SHAFT ANALYSIS at an End Point:

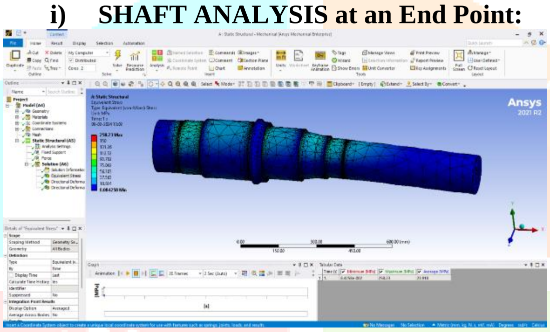

Figure-1: Equivalent Stress

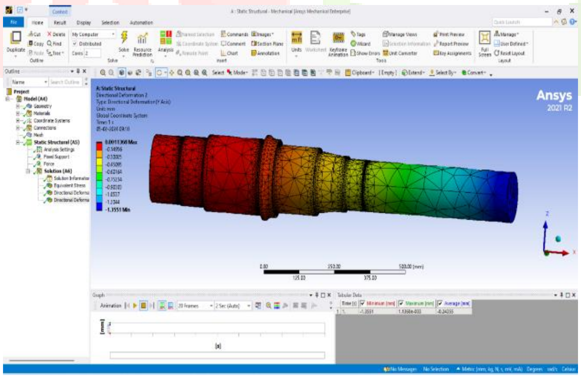

Figure-2: Directional Deformation(Y-Axis)

ii) SHAFT ANALYSIS at a Point-G:

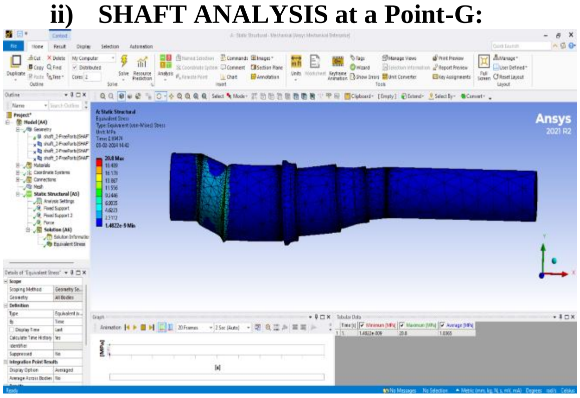

Figure-1: Equivalent Stress at Point-G

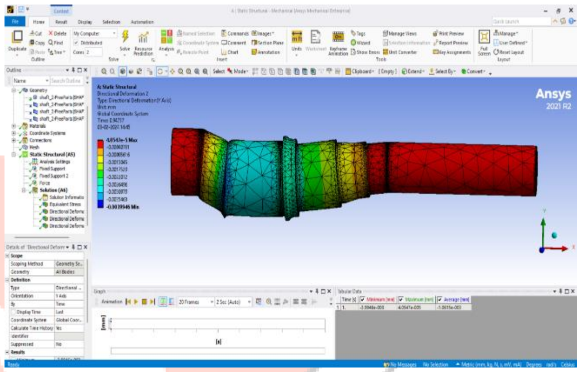

Figure-2: Directional Deformation at Point-G towards (Y-Axis)

iii) SHAFT ANALYSIS at a Point-B:

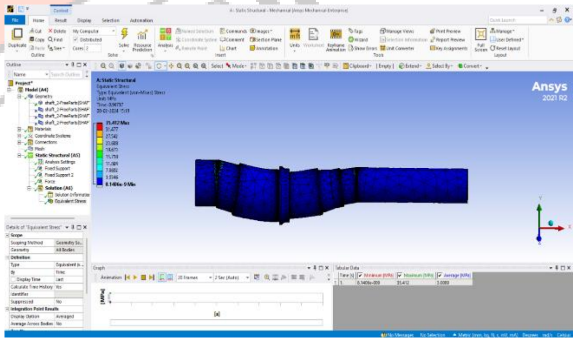

Figure-1: Equivalent Stress at Point-B

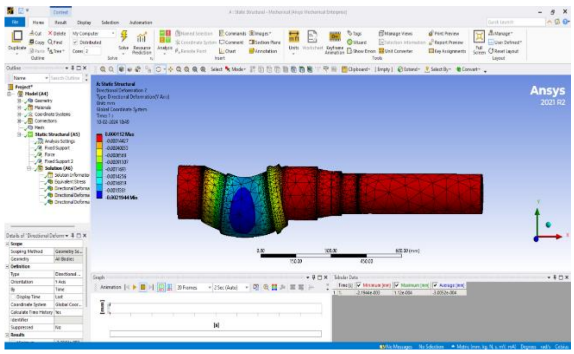

Figure-3: Directional Deformation at Point-B towards (Y-Axis)

iv) SHAFT ANALYSIS at a Point-H:

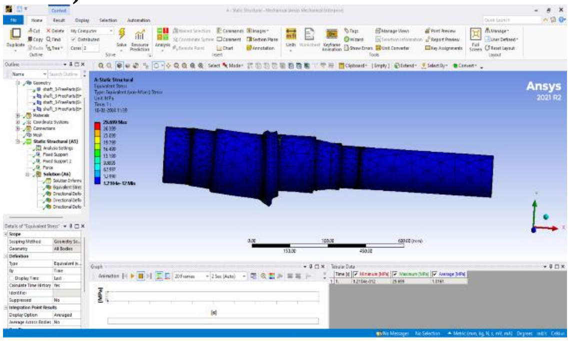

Figure-1: Equivalent Stress at Point-H

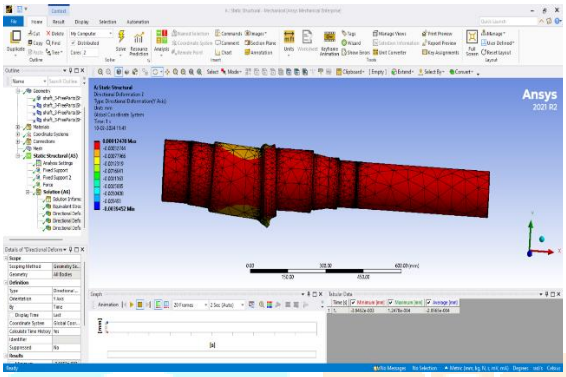

Figure-3: Directional Deformation at Point-H towards (Y-Axis)

v) SHAFT ANALYSIS at a Point-J:

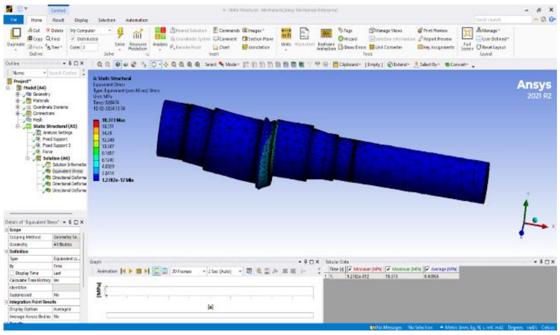

Figure-1: Equivalent Stress at Point-J

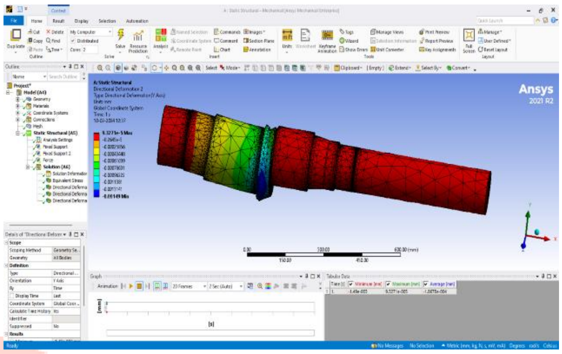

Figure-3: Directional Deformation at Point-J towards (Y-Axis)

a) ULTRASONIC TESTING:

DEPARTMENT	REPORT NO:	REPORT DATE
COKE PLANT	KPO/MED(M)/UT//E24/21	30.10.2023
COMPONENT NAME	TESTED ITEMS	ANALYSIS
SCP#03	38 No's	Ultrasonic Testing of PINS

Instrument : OLYMPUS EPOCH 650
Gain : 55-60 dB
Couplant : Grease
Frequency : 2MHz
Probe : 24mm Normal
Wave mode : Longitudinal waves
Technique : Pulse echo contact

Acceptable
Continuous Monitoring
Defective

	Description/ Location	LENGTH in mm	TEST DATE	OBSERVATIONS	STATUS
1	GTM 1 DRIVE SHAFT	1293	30.10.2023	NO ABNORMALITY OBSERVED	
2	GTM 1 NON DRIVE SHAFT	589	30.10.2023	NO ABNORMALITY OBSERVED	
3	GTM 2 DRIVE SHAFT	1293	30.10.2023	NO ABNORMALITY OBSERVED	
4	GTM 2 NON DRIVE SHAFT	590	30.10.2023	NO ABNORMALITY OBSERVED	
5	GTM 3 DRIVE SHAFT	1290	30.10.2023	NO ABNORMALITY OBSERVED	
6	GTM 3 NON DRIVE SHAFT	589	30.10.2023	NO ABNORMALITY OBSERVED	
7	GTM 4 DRIVE SHAFT	1294	30.10.2023	NO ABNORMALITY OBSERVED	
8	GTM 4 NON DRIVE SHAFT	589	30.10.2023	NO ABNORMALITY OBSERVED	
9	GTM 5 DRIVE SHAFT	1292	30.10.2023	NO ABNORMALITY OBSERVED	
10	GTM 5 NON DRIVE SHAFT	589	30.10.2023	NO ABNORMALITY OBSERVED	
11	GTM 6 DRIVE SHAFT	1292	30.10.2023	NO ABNORMALITY OBSERVED	
12	GTM 6 NON DRIVE SHAFT	590	30.10.2023	NO ABNORMALITY OBSERVED	
13	GTM 7 DRIVE SHAFT	1290	30.10.2023	NO ABNORMALITY OBSERVED	
14	GTM 7 NON DRIVE SHAFT	588	30.10.2023	NO ABNORMALITY OBSERVED	
15	GTM 8 DRIVE SHAFT	1291	30.10.2023	NO ABNORMALITY OBSERVED	
16	GTM 8 NON DRIVE SHAFT	589	30.10.2023	NO ABNORMALITY OBSERVED	
17	GTM 1 BOGGIE PIN 1	177	30.10.2023	NO ABNORMALITY OBSERVED	
18	GTM 1 BOGGIE PIN 2	176	30.10.2023	NO ABNORMALITY OBSERVED	
19	GTM 2 BOGGIE PIN 1	176	30.10.2023	NO ABNORMALITY OBSERVED	
20	GTM 2 BOGGIE PIN 2	177	30.10.2023	NO ABNORMALITY OBSERVED	
21	GTM 3 BOGGIE PIN 1	175	30.10.2023	NO ABNORMALITY OBSERVED	
22	GTM 3 BOGGIE PIN 2	176	30.10.2023	NO ABNORMALITY OBSERVED	

MOC Status (If Applicable): N/A
KPI Impacted & Delay: 1Hour of production loss.
UMC/ QAP/ Drawings: 5010A0722

H) Failure Analysis:

a) Scientific service report:

Fracture portion of shaft and NDE side bearing sent to scientific services for metallurgical analysis.
As per scientific service report it was revels that shaft was failed due to fatigue. In the counter portion the shaft was found to be in abraded condition.

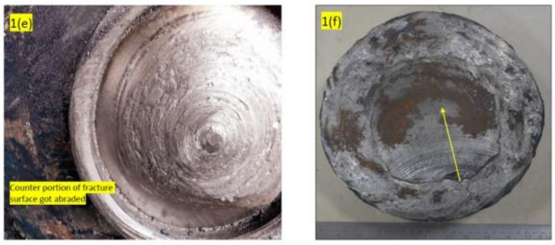

Fig 1: (e)-(f) Fracture surface of failed shaft

Material grade was closely matching with 42CrMo4, which was as per OEM design

Sample Id	Average Hardness (HV-10kg)
(K21E2001) Shaft	283
42CrMo4	280-320

Bearing collar was found spalled. Damage (roller impression) observed on raceway of bearing.
One side of collar of bearing was found more damage as compare to other.

Visual observation of failed Bearing:

Axial side

Fig 3(a): Overview of bearing referred for analysis; 3(b): Overview of bearing surface shows the race

Multiple spalling observed on the collar position of bearing outer race. Beach marks on the outer race collar confirming fatigue mode of failure of the bearing.

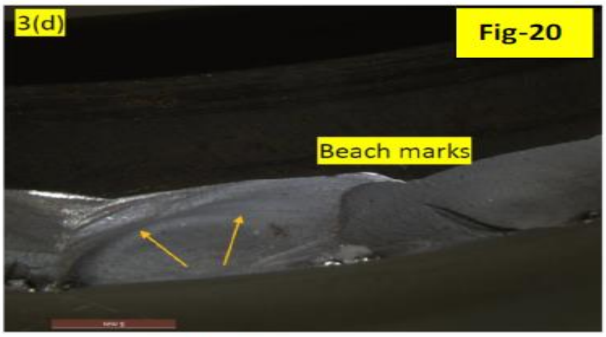

Fig 3(c): collar shows spalling from multiple location; 3(d): Spalled area at collar revealed beach marks

- The bearing attached with the shaft failed in fatigue mode due to excessive axial load on the bearing and axial shift was prominent in bearing sample.
- The roller elements seem to be unevenly loaded by observing the wear rate of the surface and also edge of the roller shows micro spalling. These indicated indicates axial loading of the bearing.

I) BEARING DESIGN DIFFERENCE:

As per OEM design it was observed that bearing should be spherical roller bearing **22240 CC/W33**, while comparing it with failed bearing, it was observed that installed bearing was **"CA/W33"** type, and it was installed during project phase.

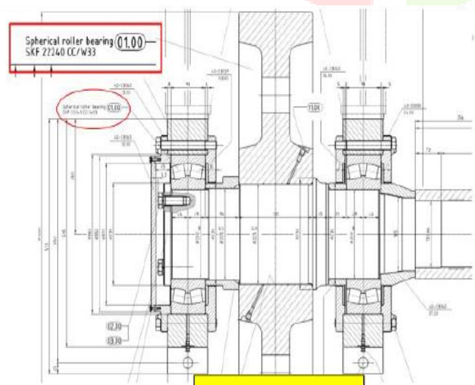

Fig.25 Bearing detail

The spherical roller bearing of the CC structure is characterized using a steel stamping cage, a reinforced symmetrical rolling body, and a movable intermediate spacer.
Compared with the CA structure, CC structure design occupies less bearing internal space than the CA structure design. By increasing the number of rolling elements and changing the outer dimensions of the rolling elements, the radial bearing capacity of the bearing can be improved to some extent.
Because the CC-type design uses a movable intermediate spacer, it can withstand greater axial load carrying capacity than the CA structural design. Both CA and CC type structural design are equivalent at the limit speed.

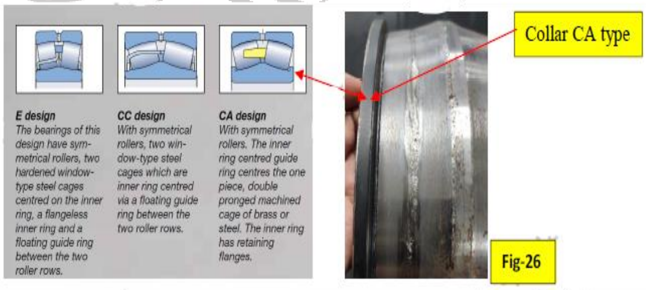

- New bearings ordered according to the UMC no. **5010A0722, it was observed that UMC was made for 22240 CC/W33 with steel cage, but in actual used bearing was 22240 CA/W33 type.**

- Installed bearings are CA type which indicates lower axial load capacity than CC type.

J) Bearing Life:

- Bearings of all drive wheels were commissioned during project phase. Recently some bearings are replaced as per ferrography report and recommendation given by MED.
- Calculation of bearing L10 life was carried out to determine the bearing self-life before failure.
- The bearing plays a crucial role in the Wheel Assembly of the SCP Machine, specifically in the Stamping, Charging, and Pushing processes.
- It is a key component responsible for bearing the main load on the shaft, with critical parameters to consider–
- Axial load on Bearing (Fa) = 2mm [10% of Fr for unknown case]
- Selected Spherical Roller Bearing No. (Make SKF) = 22240 CC/W33
- Basic Dynamic Capacity (c) = 1460KN [From Brg catalogue].
- As per calculation bearing life is more than 8 years when axial load on bearing was negligible.
- But, bearing life reduces if axial load considered as maximum allowable for the particular bearing size.

K) Conclusion:

- As per analysis it was concluded that shaft failed in bending fatigue caused by the improper alignment of bearing housing and wheel, lead to increase in axial load in shaft and hence increase in bearing clearance in drive side bearing which was un detected causing further detoriation of bearing.
- Drive side bearing failed first, and started damaging the shaft and shaft failed in early fatigue mode.
- As per bearing manufacturer allowable axial load, Fap = 0.003xBxd, where B= bearing width and d=bore dia.
- Due to excess axial load life reduced to 5.7 years. But actual axial load exerted in system was unknown.

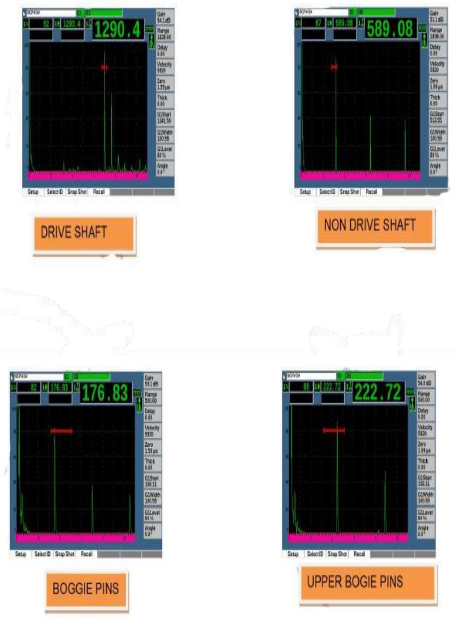

- In earlier days shaft are made of 45C8 Plain carbon steel
- Now we suggested to use 42CrMo4 alloy steel for the preparation of new shafts
- we replace the 45C8 Plain carbon steel with 42CrMo4 alloy steel because of alloy steel having more Yeild,Tensile strength and Impact strength is more compare to the plain carbon steel